Open access • Proceedings Article • DOI:10.1109/APEC.1993.290693

# Current-sourcing push-pull parallel-resonance inverter (CS-PPRI): theory and application as a fluorescent lamp driver — Source link

M. Gulko, Sam Ben-Yaakov

**Institutions:** Ben-Gurion University of the Negev

**Published on:** 07 Mar 1993 - Applied Power Electronics Conference

**Topics:** Grid-tie inverter, Inverter, Fluorescent lamp, Gas-discharge lamp and Topology (electrical circuits)

# Current-Sourcing Push-Pull Parallel-Resonance Inverter (CS-PPRI): Theory and Application as a Fluorescent Lamp Driver

Michael Gulko and Sam Ben-Yaakov*

Tel: +972-57-461561; FAX: +97257-281340; Email: SBY@BGUEE.BITNET
Department of Electrical and Computer Engineering
Ben-Gurion University of the Negev
P. O Box 653, Beer-Sheva 80105
ISRAEL

*Abstract.* **A novel topology, Current-Sourcing Push-Pull Parallel-Resonance Inverter (CS-PPRI) was investigated theoretically and experimentally. The proposed power stage is built around a current fed push-pull inverter. The main features of the proposed inverter is a load independent output current and Zero Voltage Switching (ZVS). It is suggested that the proposed CS-PPRI is a viable alternative for realizing electronic ballasts for low and high intensity discharge lamps.**

## I. INTRODUCTION

Low and high intensity discharge lamps [1] are universally recognized as the most efficient method of illumination. They require however, an extra circuitry to regulate the current thru the lamps. Electronic ballasts [1, 2] are useful not only to enable operation from a battery source, but also to facilitate dimming, to reduce the overall size of the "ballast" and to eliminate line frequency flickering [1, 3, 4]. An extra bonus of a high frequency of operation is the increase in illumination per a given electrical input power [3, 4].

Discharge lamps are an example of a family of loads that call for a current source rather than a voltage source drive. The direct approach for handling these design problems is to develop a current sourcing inverter rather than using a voltage source in series with a ballast. The objective of this study was to examine this approach by investigating a novel modification of the current fed inverter topology [5].

## II. TOPOLOGY

The proposed topology (Fig. 1) is similar to the Push-Pull Parallel-Resonance configuration described previously [6]. The basic components of this stage are an input inductor ($L_{in}$), a parallel resonance circuit ($C_r$, $L_r$) and symmetrically driven switches ($Q_1$, $Q_2$). However, unlike the classical loading method, the proposed Current-Sourcing Push-Pull Parallel-Resonance Inverter (CS-PPRI) is serially loaded. Serially coupling for a full bridge current fed inverter topology was previously described [5]. Here we present a method for a series coupling which is suitable for push-pull stages. In the proposed CS-PPRI (Fig. 1), load coupling is carried out via a current transformer which includes a split primary. The purpose of this configuration is to retain the symmetrical operation of the push-pull stage by balancing the resistive load seen by each half of the circuit.

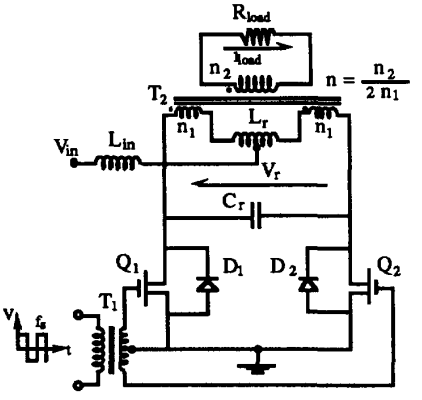


Fig. 1. The proposed Current-Sourcing Push-Pull Parallel-Resonance Inverter (CS-PPRI).

The basic operation of the proposed inverter is described by considering the equivalent circuit of the CS-PPRI (Fig. 2) in which the load is reflected to the primary and the input inductor ($L_{in}$) is replaced by a DC current source. The latter is justified by the fact that in the proposed design [6]:

$$4\,L_{in} >> L_r \qquad (1)$$

where $L_r$ is the resonant inductor. Hence, the AC current component thru $L_{in}$ will be low and therefore the input current during a resonance cycle can be considered constant.

As previously described [6], the operation of this stage when driven by a switching frequency ($f_s$) which is a lower than the resonance frequency ($f_r$), is characterized by two distinct modes: the Quasi-Resonance Mode and the Boost Mode. For each half switching frequency cycle ($f_s$), the resulting voltage waveform across the tank ($V_r$) will therefore be a quasi-sinusoidal shaped signal of ($T\lambda$) duration and zero volt during the boost period $T_{boost}$ (Fig. 3).

* Corresponding author. Incumbent of the Luck-Hille Chair of Instrumentation Design.



0-7803-0982-0/93 $3.00 1993 IEEE

In response to the voltage across the parallel resonance network, the resonant inductor current ($i_L$) and therefore the current thru the load, will be continuous and smooth (Fig. 3). Since the transitions from one mode to the other is carried out when the voltage across the tank is nil, the transistors ($Q_1$, $Q_2$) operate under Zero Voltage Switching (ZVS). This helps to reduce switching losses at high operating frequency. The experimental CS-PPRI was tested at a switching frequency range of 250 to 450 kHz.

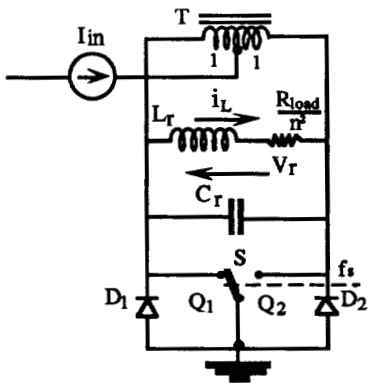


Fig. 2. Simplified equivalent circuit of the proposed CS-PPRI.

## III. ANALYSIS

*A. The Quasi-Resonant state.*

The tank voltage ($v_r$) for the quasi-resonant period ($T\lambda$, Fig. 3) can be derived by solving the following set of differential equations:

$$\frac{I_{in}}{2} = i_C + i_L \tag{2}$$

$$v_r = \frac{1}{C_r}\int i_C dt \tag{3}$$

$$v_r = L_r\frac{di_L}{dt} + i_L\frac{R_{load}}{n^2} \tag{4}$$

which were evaluated by taking into account the boundry conditions constraints: $v_r=0$ at $t=0$ and when $t=T\lambda$ (Fig. 3).

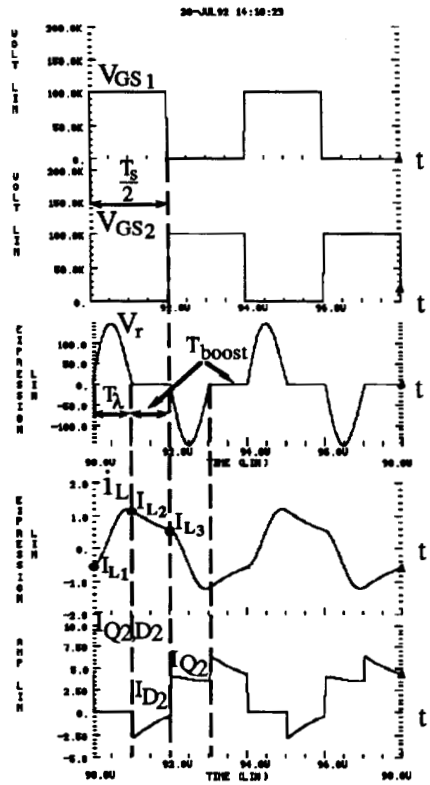


Fig.3. Expected waveforms of proposed CS-PPRI. (simulated by HSICE, MetaSoftware Co.)

$$\omega_r = \omega_o\sqrt{1-\left(\frac{1}{2Q}\right)^2}$$

$$Q = \frac{n^2}{R_{load}}\sqrt{\frac{L_r}{C_r}}$$

$$\vartheta\lambda = \omega_r T\lambda$$

$$v_r = \frac{R_{load}I_{in}}{2n^2}\left[\left(\frac{\cos(\vartheta\lambda)-e^{\frac{\vartheta\lambda R^*}{\sqrt{4-R^{*2}}}}}{\sin(\vartheta\lambda)}\right)e^{-\frac{\vartheta\lambda R^* x}{\sqrt{4-R^{*2}}}}\sin(\vartheta\lambda x) - e^{-\frac{\vartheta\lambda R^* x}{\sqrt{4-R^{*2}}}}\cos(\vartheta\lambda x) + 1\right] \tag{5}$$

where:

$R_{load}$ - Load resistor (Fig. 1).

n - Turns ratio of transformer $T_2$ (Fig. 1).

$I_{in}$ - Input current (Fig. 2).

$$\omega_o = \frac{1}{\sqrt{L_r C_r}}$$

$$R^* = \frac{1}{Q}$$ - Normalized load resistance.

$$x = \frac{t}{T\lambda}$$

At steady state conditions, the average voltage (per cycle) across $L_{in}$ is zero:

$$V_{in} - \frac{2}{T_S}\int_0^{\frac{T_S}{2}} \frac{v_r}{2}\,dt = 0 \qquad (6)$$

Applying the fact that during the $T_{boost}$ period $\{T\lambda < t < \frac{T_S}{2}\}$ (Fig. 3) $v_r = 0$:

$$V_{in} = \frac{\vartheta\lambda}{\pi\sqrt{4-R^{*2}}}\frac{f_S}{f_O}\int_0^1 v_r\,dx \qquad (7)$$

where:

$$f_O = \frac{\omega_O}{2\pi}$$

Integrating (7), assuming that the SC-PPRI is lossless and equating input to output power, we obtain:

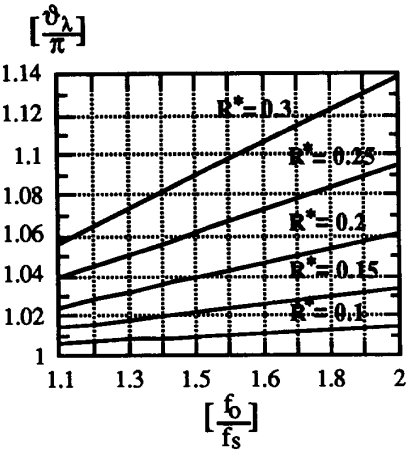


Fig. 4. The normalized quasi-resonant period ( $\frac{\vartheta\lambda}{\pi} = 2f_rT\lambda$) as a function of the normalized switching frequency ($f_O/f_S$) with the normalized load ($R^*$) as a parameter.

$$I^*_{load} = \frac{2}{R^*}\left[\frac{\frac{2\pi\,Sin(\vartheta\lambda)}{\sqrt{4-R^{*2}}}}{\left(\frac{4}{4-R^{*2}}\right)\vartheta\lambda\,Sin(\vartheta\lambda)+2Cos(\vartheta\lambda)-\left(e^{\frac{\vartheta\lambda R^*}{\sqrt{4-R^{*2}}}}+e^{-\frac{\vartheta\lambda R^*}{\sqrt{4-R^{*2}}}}\right)}\frac{f_O}{f_S}\right]^{\frac{1}{2}} \qquad (8)$$

where:

$I^*_{load} = I_{load\,(r.m.s)}\frac{n}{V_{in}}\sqrt{\frac{L_r}{C_r}}$ - Normalized load current.

Utilizing the fact that the resonant inductor current ($i_L$) is symmetrical (Fig. 3) and that it decays expotentialy during the boost period (Fig. 3), from (2) and (3),we find (9):

Applying now (9), the fact that the boundry conditions as: $i_L=I_{L1}$ at t=0 (x=0) and $i_L=I_{L2}$ when t= $T\lambda$ (x=1) (Fig. 3) and the expotential behavior of the inductor current ($i_L$), the frequency ratio ($f_O/f_S$) is expressed in (10):

$$i_L = \frac{I_{in}}{2}\left[1-\frac{R^*\sqrt{4-R^{*2}}}{2}e^{-\frac{\vartheta\lambda R^* x}{\sqrt{4-R^{*2}}}}\left(\left(\frac{Cos(\vartheta\lambda)-e^{\frac{\vartheta\lambda R^*}{\sqrt{4-R^{*2}}}}}{Sin(\vartheta\lambda)}\right)\left(Cos(\vartheta\lambda x)-\frac{R^*Sin(\vartheta\lambda x)}{\sqrt{4-R^{*2}}}\right)+\frac{R^*Cos(\vartheta\lambda x)}{\sqrt{4-R^{*2}}}+Sin(\vartheta\lambda x)\right)\right] \qquad (9)$$

$$\frac{f_O}{f_S} = \frac{2}{\pi R^*}\left[\frac{1}{2}\ln\left(-\frac{(2-R^{*2})Sin(\vartheta\lambda)+R^*\sqrt{4-R^{*2}}\left(Cos(\vartheta\lambda)-e^{-\frac{\vartheta\lambda R^*}{\sqrt{4-R^{*2}}}}\right)}{(2-R^{*2})Sin(\vartheta\lambda)-R^*\sqrt{4-R^{*2}}\left(Cos(\vartheta\lambda)-e^{\frac{\vartheta\lambda R^*}{\sqrt{4-R^{*2}}}}\right)}\right)-\frac{\vartheta\lambda R^*}{\sqrt{4-R^{*2}}}\right] \qquad (10)$$

The last expression can be used to explore the dependence of the quasi-resonant period ($T\lambda$) on the switching frequency ($f_S$) and load ($R_{load}$) (Fig. 4). It is evident that under the operating conditions discussed here, the quasi-resonant period is longer than half the period of the natural resonant frequency ($f_O$).

*B. Voltage stress.*

Assuming that the voltage waveform $v_r$ (Fig. 3) could be approximated by a sinusoidal wavefom [6], and apllying (7), we find the maximun tank voltage ($V_{rm}$ ) which is the voltage stress of the transistors ($V_{Qm}$) and the diodes ($V_{Dm}$):

$$V_{Qm} = V_{Dm} = V_{rm} = \frac{V_{in}\pi^2\sqrt{4-R^{*2}}}{2\vartheta\lambda}\,\frac{f_o}{f_s} \qquad (11)$$

*C. Current stress.*

The maximum normalized transistor current ($I^*_{Qm}$) (Fig. 5) was found to be:

$$I^*_{Qm} = I_{Qm}\frac{\omega_o L_r}{V_{in}} = I^{*2}_{load}R^*\left(\frac{1}{2}+\frac{1}{4\,Sin(\vartheta\lambda)}\left[(2-R^{*2})Sin(\vartheta\lambda)+R^*\sqrt{4-R^{*2}}\left(Cos(\vartheta\lambda)-e^{-\frac{\vartheta\lambda R^*}{\sqrt{4-R^{*2}}}}\right)\right]\right) \qquad (12)$$

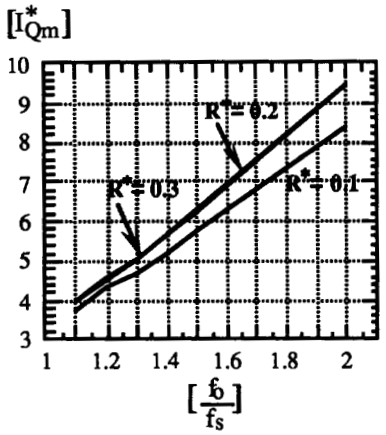


Fig. 5. Normalized transistor current ($I^*_{Qm}$) as a function of the normalized switching frequency ($f_O/f_S$) with the normalized load ($R^*$) as a parameter.

The maximum normalized diode current ($I^*_{Dm}$) (Fig. 6) was derived as:

$$I^*_{Dm} = I_{Dm}\frac{\omega_o L_r}{V_{in}} = I^*_{Qm} - I^{*2}_{load}R^* \qquad (13)$$

The transistors' normalized r.m.s. current $I^*_{Qr.m.s}$ was evaluated and is shown in Fig. 7 where:

$$I^*_{Qr.m.s} = I_{Qr.m.s}\frac{\omega_o L_r}{V_{in}} \qquad (14)$$

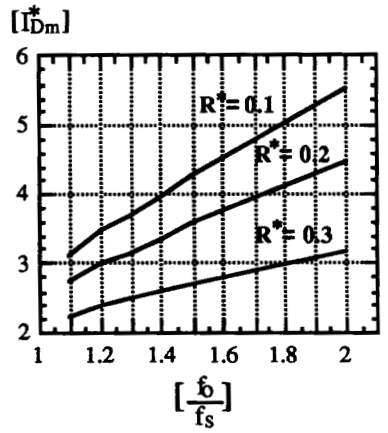


Fig. 6. Normalized diode current ($I^*_{Dm}$) as a function of the normalized switching frequency ($f_O/f_S$) with the normalized load ($R^*$) as a parameter.

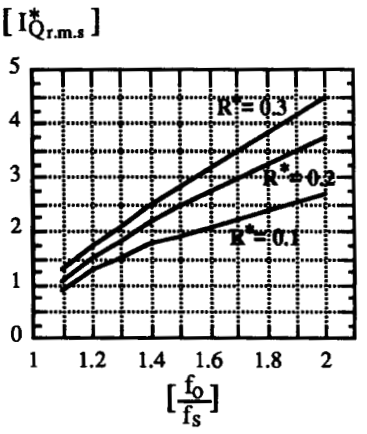


Fig. 7. Normalized r.m.s transistor current ($I^*_{Qr.m.s}$) as a function of the normalized switching frequency ($f_O/f_S$) with the normalized load ($R^*$) as a parameter.

## IV. EXPERIMENTAL RESULTS

The design parameters of the experimental CS-PPRI were as follows:
$V_{in}$=24V; $L_{in}$= 70 μH; $C_r$=8.24 nF; n=4; $f_O$=487.9 kHz; $L_r$=12.9 μH (including 1.6 μH of leakage inductor of the transformer $T_2$)

The waveform of the experimental circuit (Fig. 8) were found to be smooth and indicative of ZVS (Fig. 3). The

parasitic oscillation of the current thru the switch is partially due to a layout modification required to facilitate current measurements ( an extra loop at the drain of one of the transistors). It should be pointed out though, that a slight parasitic oscillation does not interfere with the inherent ZVS of the proposed CS-PPRI. The smooth operation of the CS-PPRI dispose of the need to use snubbers or clamps.

The output current for various load resistances (Fig. 9) were found to be in good agreement with the analytical expected values (8). The somewhat larger discrepancy at high frequency ratios ($f_O/f_S$) is due to conductive losses which increase as the boost period is becoming longer. Since parasitic losses were ignored in the present theoretical analysis, one would expect an inconsistency between the analytical and experimental results when the losses are high.

The theoretical and experimental results clearly point out to the fact that the proposed CS-PPRI is operating as a current source (Fig. 9) and that the magnitude of the output current is controlled by the driving switching frequency ($f_S$) (Fig. 10).

The overall efficiency of the experimental CS-PPRI was found to be around 85% for a power level of 80 Watt.

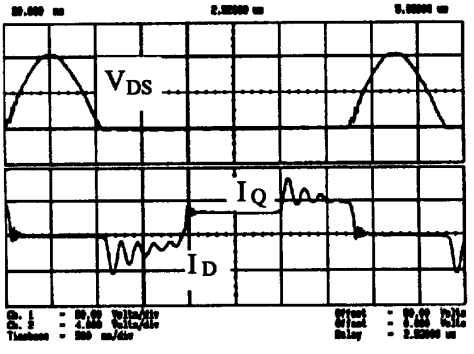


(a)

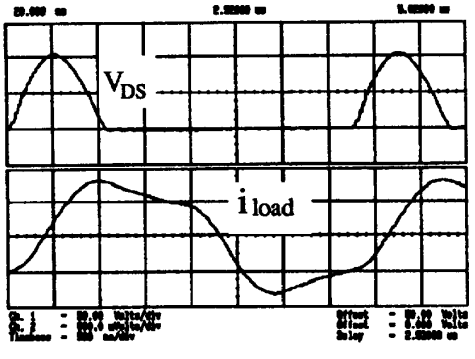


(b)

Fig. 8. Measured waveforms of experimental CS-PPRI.Vertical scales 50V/div, 2A/div in (a) and 0.6 A/div in (b). Horizontal scales: 500 nS/div.

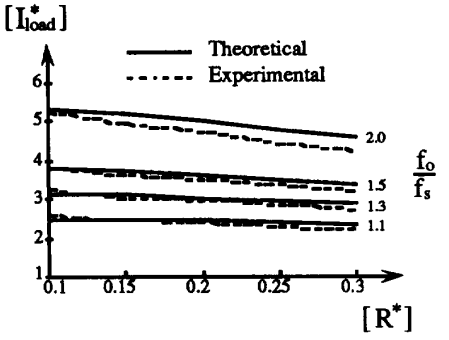


Fig. 9. The relationship between the normalized output current $I^*_{load}$ (equation 8) and the normalized load resistance $R^*$ (equation 10) as a function of the frequency ratio ($f_O/f_S$).

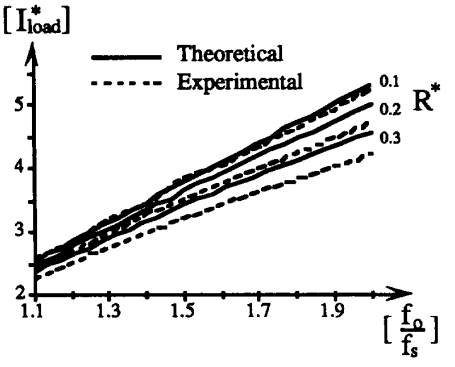


Fig. 10. The relationship between the normalized output current $I^*_{load}$ (equation 8) and the frequency ratio ($f_O/f_S$) as a function the normalized load resistance $R^*$ (equation 10 ).

## V. APPLICATION AS A FLUORESCENT LAMP DRIVER

The current sourcing nature of the proposed CS-PPRI makes it a viable alternative for fluorescent lamp driver. The proposed modification for a battery operated fluorescent lamp driver is shown in Fig. 11. The main difference of this driver as compared to the one shown in Fig. 1, is the inclusion of an extra capacitor ($C_{ig}$) at the output side. The purpose of this capacitor is to provide initial filament heating path and high voltage during the lamp starting period [1]. The value of the extra capacitor ($C_{ig}$, Fig. 11) can be calculated by solving the set of non-linear equations for no load condition given in [7].

As previously documented [1, 3], fluorescent lamps exhibit a resistive nature at high frequencies. This can be clearly seen by examining the experimental lamp voltage and current depicted in Fig. 12. It is thus evident that a first order approximation of a fluorescent lamp, when driven by a high frequency source, is a pure resistor. The present study reveals

that this average resistance can be desribed by a simple model which is readily interpreted is physical terms.

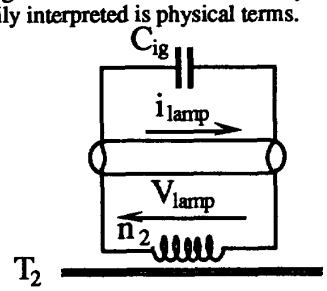


Fig. 11. Output section of the CS-PPRI (Fig. 1) when used as a battery operated fluorescent lamp driver.

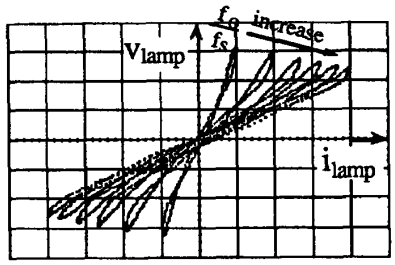


Fig. 12. Measured V-I characteristic of the experimental fluorescent lamp (General Electric type F40D/2 ) as a function the frequency ratio $f_o/f_s$ ($f_o/f_s$ range: 1.1-1.5). Vertical scale: 50 V/div. Horizontal scale: 0.2 A/div. Nominal switching frequency 300 kHz.

The proposed model is based on our observation (Fig. 12) that the V-I characteristic of a fluorescent lamp when driven by a sinusoidal current is characterized by the following relationship:

$$I_{pk}(R_{eq} + R_S) = V_{max} \quad (14)$$

or:

$$\sqrt{2}\, I_{r.m.s}(R_{eq} + R_S) = V_{max} \quad (15)$$

where $R_{eq}$ is the (dynamic) equivalent resistance of the lamp, $I_{pk}$ is the peak current thru the lamp, $V_{max}$ is a constant of the lamp (akin to the breakdown voltage) and $R_S$ is a series resistance. Equation (15) can be written as:

$$R_{eq} = \frac{V_{max}}{\sqrt{2}\, I_{r.m.s}} - R_S \quad (16)$$

where $V_{max}$ and $R_S$ are constants of the lamp. The experimental parameters $V_{max}$ and $R_S$ can be evaluated by fitting a linear curve to the top of the family curves shown in Fig. 12. The line can be defined by two peak points ($V_{pk.1}$,$I_{pk.1}$), ($V_{pk.2}$,$V_{pk.2}$) (Fig. 13) to yield:

$$R_S = \mathrm{Tan}(\beta) = \frac{V_{pk.1} - V_{pk.2}}{I_{pk.2} - I_{pk.1}} \quad (17)$$

$$V_{max} = R_S I_{pk.1} + V_{pk.1} \quad (18)$$

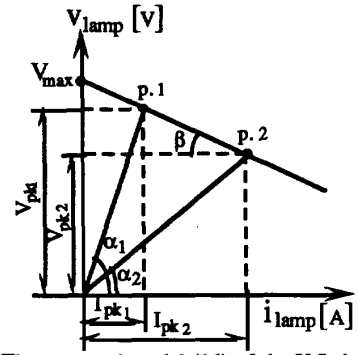


Fig. 13. The proposed model (16) of the V-I characteristic of a fluorescent lamp, when driven by a high frequency sinusoidal current source. See text for details.

Excellent agreement was found between measured data and $R_{eq}$ estimation by (16) (Fig. 14)

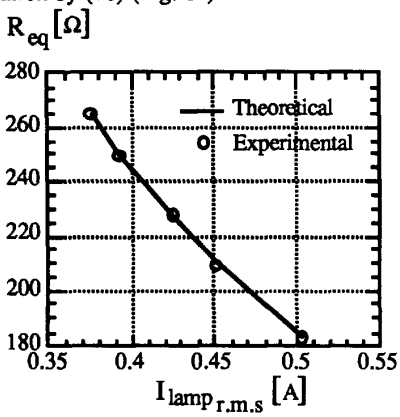


Fig. 14. The relationship between the (dynamic) equivalent resistance of the lamp ($R_{eq}$) and the lamp current ($I_{lamp\ (r.m.s)}$). The parametrs (16) of the experimental fluorescent lamp (General Electric type F40D/2 (40W)): $R_S$ = 58.66Ω, Vmax = 121.5V.

A simple interpretation to the experimantally derived equation (16) is that the familiar low frequency V-I curve of the fluorescent lamp [1] represents steady state relationship between the voltage across the lamp and the space charge along it. At high enough frequency, the space charge density does not decay appreciably within one cycle. Consequently at high frequencies, the lamp represents a pure resistor whose value is a function of the average space charge density. The value of this resistor is thus inversly proportional to the current thru the lamp (16) and is influenced by the fact that the steady state voltage across the lamp drops as the current thru it increases [1].

*A. Design guidelines.*

The following procedure is suggested for the practical design of the CS-PPRI driver for a fluorescent lamp of a given input voltage ($V_{in}$), current ($I_{lamp\ (r.m.s)}$) and power ($P_{lamp}$):

1. Select the switching frequency ($f_s$) according to the transistors and magnetic material available.
2. Choose ($R^*$) to be in the range 0.1 to 0.2 (Fig. 7).
3. Select the ratio ($f_o/f_s$) to be in the range 1.1 to 1.5 (Fig. 7).
4. Calculate the apparent load resistor ($R_{load}$):

$$R_{load} = \frac{P_{lamp}}{\eta\, I^2_{lamp(r.m.s)}}$$

where $\eta$ - the efficiency of the CS-PPRI (0.8-0.85).

5. Calculate the natural resonant frequency ($f_o$) from the ratio ($f_o/f_s$).
6. Select $I^*_{load}$ from Fig. 9 for the chosen $R^*$, ($f_o/f_s$).
7. Calculate ($L_r$):

$$L_r = \frac{\left(\frac{I^*_{load}\, V_{in}}{I_{lamp(r.m.s)}}\right)^2 \frac{R^*}{R_{lamp}}}{\omega_o}$$

where $\omega_o = 2\pi f_o$

8. Calculate (n): $n = \dfrac{I^*_{load}\, V_{in}}{I_{lamp(r.m.s)}\omega_o L_r}$
9. Calculate ($C_r$): $C_r = \dfrac{1}{L_r\, \omega_o{}^2}$
10. Estimate the current stress of the transistors ($I_{Qm}$) and anti-parallel diodes ($I_{Dm}$) from (12), (13) and Figs. 5 and Fig. 6.
11. Calculate the voltage stress of the transistors ($V_{Qm}$) and anti-parallel diode ($V_{Dm}$) from equation (11).
12. The design of ($L_r$) is based on the inductance ($L_r$), maximum voltage ($V_{rm}$), r.m.s. current ($I_{Lr(r.m.s)}$) and switching frequency ($f_s$):

$$I_{Lr(r.m.s)} = \sqrt{\left(I_{lamp(r.m.s)}{}^n\right)^2 + \left(0.5\frac{V_{in} I^{*2}_{load} R^*}{\omega_o L_r}\right)^2}$$

13. Similarily, transformer ($T_2$) design is based on the maximum transformer voltage ($V_{Trmax}$) and current ($I_{Tr(r.m.s)}$):

$$V_{Trmax} = \frac{V_{in}}{\omega_o L_r}\left(I^*_{Qm} - 0.5 I^{*2}_{load} R^*\right)\frac{R_{lamp}}{n^2}$$

$$I_{Tr(r.m.s)} = I_{Lr(r.m.s)}$$

14. Choose ($L_{in}$) such that $4L_{in} >> L_r$. Calculate the maximum inductor voltage ($V_{Linmax}$) and the inductor current ($I_{Lin(r.m.s)}$):

$$V_{Linmax} = \frac{V_{rm}}{2} - V_{in}$$

$$I_{Lin(r.m.s)} = I_{in(dc)} = \frac{V_{in} I^{*2}_{load} R^*}{\omega_o L_r}$$

These constraints normally call for an air gapped construction.

15. The resonant capacitor ($C_r$) must be capable of sustaining the expected maximum voltage ($V_{Crmax} = V_{rm}$) and should have a low ESR.

## VI. CONCLUSIONS

The results of the present study suggest that the CS-PPRI is a viable alternative for the realization of high frequency current sources. The inherent ZVS characteristic of the proposed topology permits efficient operation at high frequency, possibly to 1MHz, with commercially available electronic devices and magnetic materials. The proposed CS-PPRI is particularly useful as a driver for discharge lamp which need to be fed by a current source. The advantage of this approach over previously described topologies is that it eliminates the need for an extra (inductive or capacitive) ballast. That is, there is no need to generate a much higher voltage and then to limit the current by a series impedance. In the proposed CS-PPRI the current is a function of the frequency ratio ($f_o/f_s$), a feature that can be used to realize a fluorescent lamp dimmer. The proposed model for the resistance of a fluorescent lamp can be useful in the design of electronic ballasts for these non linear devices.

## REFERENCES


[1] W. Elenbaas, Ed., *Fluorescent Lamps*, Macmillan, London, 1971.

[2] J. Spangler, B. Hussain, A. K. Behera, "Electronic Fluorescent Ballast using a Power Factor Correction Techniques for Loads Greater Than 300 Watts," *APEC-91*, pp.393-399, March, 1991.

[3] E. E. Hammer, "High Frequency Characteristics of Fluorescent Lamp up to 500 kHz," *Journal of the Illuminating Engineering Society*, pp.52-61, Winter, 1987.

[4] W. R. Alling, "Important Design Parameters for Solid-State Ballasts," *IEEE Transactions on Industry Applications*, Vol. 25, No. 2, pp. 203-207, March/April, 1989.

[5] D. V. Divan, "Design Considerations for Very High Frequency Resonant Mode DC/DC Converters," *IEEE Transactions on Power Electronics*, Vol. Pe-2, No.1, pp. 45-54, January, 1987.

[6] G. Ivensky, A. Abramovitz, M. Gulko and S. Ben-Yaakov, "A Resonant DC-DC Transformer,"*IEEE Transactions on Aerospace Electronic Systems* (in press).

[7] G. Ivensky, M. Gulko and S. Ben-Yaakov, "Current-Fed Multi-Resonant DC-DC Converter,"*APEC-93* (this proceedings).